

# Galactic Halo Models and Particle Dark-Matter Detection

Marc Kamionkowski\* and Ali Kinkhabwala†

*Department of Physics, Columbia University, 538 West 120th Street, New York, New York 10027*

(October 1997)

Rates for detection of weakly-interacting massive-particle (WIMP) dark matter are usually carried out assuming the Milky Way halo is an isothermal sphere. However, it is possible that our halo is not precisely spherical; it may have some bulk rotation; and the radial profile may differ from that of an isothermal sphere. In this paper, we calculate detection rates in observationally consistent alternative halo models that produce the same halo contributions to the local and asymptotic rotation speeds to investigate the effects of theoretical uncertainty of the WIMP spatial and velocity distribution. We use self-consistent models to take into account the effects of various mass distributions on the local velocity distribution. The local halo density may be increased up to a factor of 2 by flattening or by an alternative radial profile (which may also decrease the density slightly). However, changes in the WIMP velocity distribution in these models produce only negligible changes in the WIMP detection rate. Reasonable bulk rotations lead to only an  $O(10\%)$  effect on event rates. We also show how the nuclear recoil spectrum in a direct-detection experiment could provide information on the shape and rotation of the halo.

98.70.V, 98.80.C

CU-TP-864, CAL-648, hep-ph/9710337

## I. INTRODUCTION

Perhaps the most intriguing explanation for the dark matter in the Galactic halo is that it is composed of weakly-interacting massive particles (WIMPs) [1]. These particles typically have masses between 10 GeV and a few TeV and couple to ordinary matter only with electroweak-scale interactions. For example, the leading candidate WIMP is perhaps the neutralino, the lightest superpartner in supersymmetric extensions of the standard model [2]. Several complementary efforts are currently afoot to detect these halo dark-matter particles. For many WIMP candidates, the most promising avenue is direct detection of the  $O(10\text{ keV})$  recoil energy deposited in a low-background laboratory detector when a halo WIMP scatters from a nucleus therein [3,4]. Another promising technique for many other WIMP candidates is detection of the energetic neutrinos produced by annihilation of WIMPs which have been captured in the Sun and/or Earth [5]. There are also efforts to detect anomalous cosmic-ray positrons, antiprotons, and gamma rays which may have been produced by WIMP annihilation in the Galactic halo (see Ref. [1] for a review and further references).

The predicted rates for all of these techniques depend on the mass and interactions of the WIMP. The rates for scattering from nuclei also depend on quantities such as quark densities in the nucleon and on nuclear form factors. Considerable efforts have been made to survey the plausible parameter space for supersymmetric WIMPs. Furthermore, the sources of uncertainty in the predicted direct-detection and energetic-neutrino rates from, e.g., quark densities and nuclear form factors have been evaluated and isolated.

Of course, predictions depend on the spatial and velocity distribution of WIMPs in the halo. In most (all?) calculations of dark-matter detection rates, the halo is

assumed to be a cored isothermal sphere parameterized by a central (or alternatively, local) density and core radius which are fit to the observationally inferred halo contribution to the rotation curve. In this model, the velocity distribution is Maxwell-Boltzmann with a velocity dispersion determined by the rotation speed at large radii. Observational uncertainties in the rotation curve and in the disk and bulge contributions lead roughly to a factor-of-two uncertainty in the local dark-matter density. Assuming an isothermal sphere, one finds the local dark-matter density  $\rho_0 = 0.2 - 0.4 \text{ GeV cm}^{-3}$  and a velocity dispersion  $\bar{v} = 270 \pm 70 \text{ km sec}^{-1}$ .

In addition to these uncertainties from the rotation curve and disk mass distribution, deviations from the standard nonrotating isothermal spherical halo are also plausible, if not probable. Essentially all the empirical information we have on the halo is provided by the rotation curve. To a first approximation, almost any halo mass distribution which gives rise to a flat rotation curve is acceptable. Although there are some arguments that the halo must be more diffuse than the disk [6], there is no reason why it should be perfectly spherical. In fact, there is ample evidence that the halos of several external spiral galaxies are flattened by roughly a factor of two [7] and now some evidence that the Milky Way halo is similarly flattened [8]. The dominant effect of flattening on the detection rate is through the local dark-matter density [9]. However, flattening may also affect detection rates through the velocity distribution, which has not been taken into account.

Bulk rotation can also affect the velocity distribution of WIMPs seen at the Earth. Again, the rotation curve is determined by the halo mass distribution and is insensitive to its velocity distribution. Therefore, there is no empirical evidence to rule out a halo with some bulk rotation. Although there are theoretical arguments against a rotation-dominated velocity distribution, there are also

reasons to expect the halo to have some bulk rotation [10,11].

There may also be theoretical uncertainties in the halo radial profile. The functional form for the radial profile commonly assumed is in fact a phenomenological model which produces a linearly rising rotation curve at small radii and a flat rotation curve at large radii. There are other radial profiles which will satisfy these requirements and produce the same rotation speeds at the Galactocentric and large radii to which the models are fit.

In this paper, we investigate uncertainties in the WIMP detection rate which arise from imprecise knowledge of the spatial and velocity distribution of dark-matter particles. To do so, we use a class of self-consistent models for a flattened and/or rotating halo which have been developed by Evans [12], and consider several plausible spherical distributions. All the models we consider produce the same halo contribution to the local and asymptotic rotation speeds. Some of our models may appear to be extreme (in terms of flattening, bulk rotation, or central density) to some Galactic-dynamics experts; however, our primary aim is to provide a *conservative* estimate of the uncertainty in dark-matter detection rates from uncertainties in the halo distribution, and the models we consider span a range of observationally plausible—though not necessarily theoretically favored—models.

We find that flattening and/or changes to the radial profile may increase the density by roughly a factor of two. However, either departure from the canonical isothermal sphere has a negligible effect on the velocity-distribution dependence of the event rate. The bulk rotations which may arise in realistic galaxy-formation scenarios will have no more than a 10% effect on detection rates.

In the next Section, we review the procedure for calculating detection rates. In Section III, we review the distribution functions for the Evans models which we use to investigate the effects of flattening and bulk rotation. Results for the effects of flattening on the local WIMP velocity distribution, density, and total and differential detection rates are provided in Section IV. We also propose here that the measured differential recoil-energy distribution (in case of detection) could be used to constrain the bulk rotation and flattening of the halo. In Section V we investigate the effects of uncertainties in the halo radial profile in spherical models on dark-matter detection rates. In Section VI we summarize and make some concluding remarks. We also discuss how rates for indirect detection of WIMPs will be affected in these alternative halo models.

## II. CALCULATING DIRECT-DETECTION RATES

One can write the differential rate for direct WIMP detection [1] as

$$\frac{dR}{dQ} = \frac{\sigma_0 \rho_0}{2m_\chi m_r^2} F^2(Q) \int_{v_{\min}}^{\infty} \frac{f_1(v)}{v} dv, \quad (2.1)$$

where  $\sigma_0$  is the cross-section (at zero momentum transfer);  $\rho_0$  is the local dark matter density;  $m_r$  is the reduced mass  $m_N m_\chi (m_N + m_\chi)^{-1}$ , where  $m_N$  is the mass of a target nucleus and  $m_\chi$  is the WIMP mass;  $Q = |\mathbf{q}|^2/2m_N$  is the deposited energy, where  $\mathbf{q}$  is the momentum transfer;  $F(Q)$  is a nuclear form factor;  $f_1(v)$  is the distribution of WIMP speeds relative to the detector (normalized to 1); and  $v_{\min} = [(Qm_N)/(2m_r^2)]^{1/2}$ . Defining the dimensionless quantity,

$$T(Q) = \frac{\sqrt{\pi}}{2} v_0 \int_{v_{\min}}^{\infty} \frac{f_1(v)}{v} dv, \quad (2.2)$$

and taking  $F(Q) = \exp(-Q/2Q_0)$ , the differential detection rate can be written as

$$\frac{dR}{dQ} = \left( \frac{\rho_0 \sigma_0}{\sqrt{\pi} v_0 m_\chi m_r^2} \right) \exp(-Q/Q_0) T(Q); \quad (2.3)$$

i.e., the density times a velocity-dependent term. The total event rate can be determined by integrating over all detectable energies:

$$R = \int_{E_T}^{\infty} \frac{dR}{dQ} dQ, \quad (2.4)$$

where  $E_T$  is the threshold energy for the detector.

## III. HALO MODELS

To study the effects of flattening and bulk rotation on detection rates, we use Evans's family of analytic axisymmetric distribution functions (DFs) [12],

$$F(E, L_z^2) = [AL_z^2 + B] \exp(4E/v_0^2) + C \exp(2E/v_0^2), \quad (3.1)$$

with

$$A = \left( \frac{2}{\pi} \right)^{5/2} \frac{(1-q^2)}{Gq^2 v_0^3}, \quad B = \left( \frac{2}{\pi^5} \right)^{1/2} \frac{R_c^2}{Gq^2 v_0}, \quad C = \frac{2q^2 - 1}{4\pi Gq^2 v_0}, \quad (3.2)$$

where  $E$  is the binding energy,  $L_z$  is the azimuthal component of angular momentum,  $v_0$  is the circular speed at large radii,  $R_c$  is the core radius, and  $q$  is the flattening parameter, ranging from  $q = 1$  for a cored, spherical halo to  $q = 1/\sqrt{2} \approx 0.707$  for the most flattened non-negative DF [12]. These models elegantly reproduce Binney's potential and corresponding density [13],

$$\psi(R, z) = -\frac{1}{2} v_0^2 \log \left( R_c^2 + R^2 + \frac{z^2}{q^2} \right), \quad (3.3)$$

$$\rho(R, z) = \frac{v_0^2}{4\pi G q^2} \frac{(2q^2 + 1)R_c^2 + R^2 + (2 - q^{-2})z^2}{(R_c^2 + R^2 + z^2 q^{-2})^2}, \quad (3.4)$$

where  $R$  is the radial distance and  $z$  is the vertical distance above the disk. These are suitable for describing the halo since they produce rotation curves which rise linearly at small radii and are flat at large radii.

In this calculation, we take the dark-matter contribution to the local circular velocity to be  $v_c(R_0) = 170$  km sec<sup>-1</sup> (which we get from a local rotation speed of 220 km sec<sup>-1</sup> and a disk contribution of 140 km sec<sup>-1</sup>),  $v_0 = v_\infty = 220$  km sec<sup>-1</sup>, a Galactocentric radius  $R_0 = 8.5$  kpc, and  $z = 0$  kpc. The core radius  $R_c$  is obtained by noting that in the plane  $z = 0$ ,

$$v_c^2 = R \frac{d\psi}{dR} = \frac{v_0^2 R^2}{R_c^2 + R^2}. \quad (3.5)$$

Therefore, for all  $q$ , the core radius is

$$R_c = R_0 \left( \frac{v_\infty^2}{v_c(R_0)^2} - 1 \right)^{1/2} \approx 7 \text{ kpc}. \quad (3.6)$$

[We have checked that our conclusions on the effects of flattening are unchanged if we adopt other plausible values for  $v_\infty$ ,  $v_c(R_0)$ , and  $R_0$ .]

The isopotential contours for these models are ellipsoidal with (short-to-long) axis ratios  $q$  [c.f., Eq. (3.3)]. Fig. 1 shows isodensity contours for  $q = 1, 0.85$ , and  $1/\sqrt{2} \approx 0.707$  (for  $R_c = 7$  kpc). The isodensity contours are not ellipsoidal. For small radii, they are close to spherical, and they become more flattened for larger radii. Inspection of Fig. 1 shows that (for  $R_c = 7$  kpc) the short-long axis ratio for the isodensity contours is roughly 1:2 for  $q \simeq 0.707$  for radii comparable to our Galactocentric radius.

The DFs above have no bulk rotation. However, a family of DFs with bulk rotations can be constructed by considering linear combinations,

$$G(E, L_z) = aF_+(E, L_z) + (1 - a)F_-(E, L_z), \quad (3.7)$$

of DFs

$$F_+(E, L_z^2) = \begin{cases} F(E, L_z^2), & v_\phi > 0; \\ 0, & v_\phi < 0, \end{cases} \quad (3.8)$$

$$F_-(E, L_z^2) = \begin{cases} 0, & v_\phi > 0; \\ F(E, L_z^2), & v_\phi < 0, \end{cases} \quad (3.9)$$

with only positive or negative azimuthal-velocity components  $v_\phi$ . These models have the same spatial distributions as the nonrotating models  $F(E, L_z)$ . The parameter  $a$  ranges from 1 (for maximal corotation) to 0.5 (the model with no net rotation) to 0 (maximal counterrotation), and is related to the dimensionless spin parameter  $\lambda$  usually used to quantify galactic angular momenta by  $\lambda = 0.36|a - 0.5|$ .

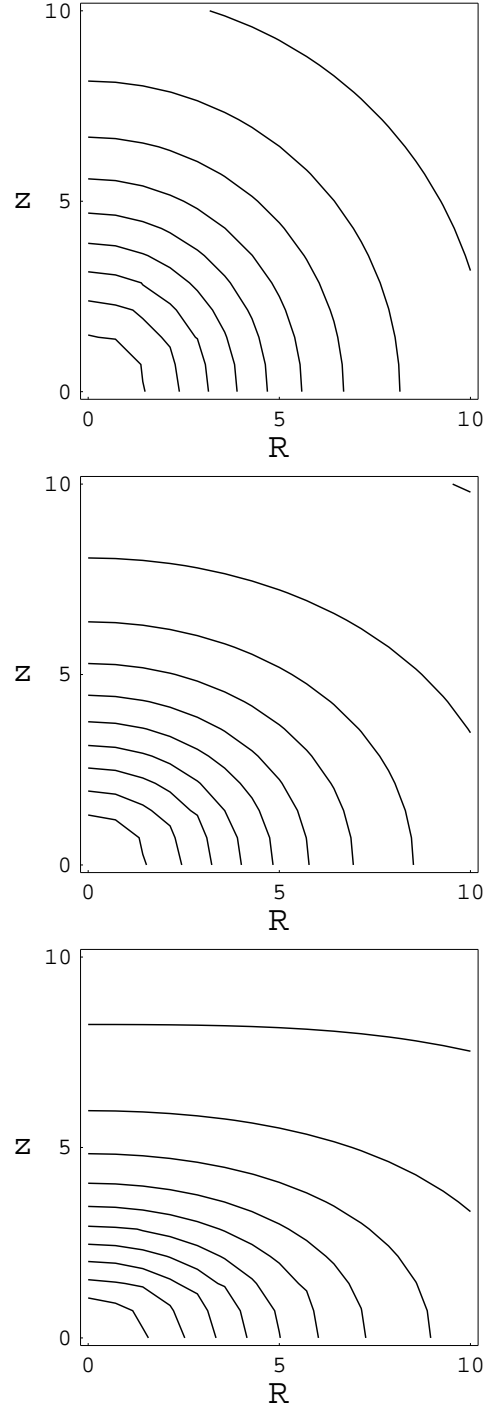


FIG. 1. Halo isodensity contours for the Evans models for  $q = 1, 0.85, 0.707$ , where the  $z$  and  $R$  axes are in kpc.)

The DFs discussed so far specify the velocity distribution in the Galactic rest frame. However, the solar system moves with respect to this frame with a velocity  $v_s = 220$  km sec<sup>-1</sup>. Therefore, the DF  $F_s(v_R, v_z, v_\phi)$  with respect to the Earth can be obtained from the rest-frame DF  $F$  by substituting  $v_\phi \rightarrow v_\phi + v_s$ .

### A. No Net Rotation

For these models, the distribution function is even in the variable  $v_\phi$ ; there are as many particles circling around clockwise as there are counterclockwise.

Substituting the binding energy,

$$E = -\frac{1}{2}v^2 - \frac{1}{2}v_0^2 \log \left( R_c^2 + R^2 + z^2/q^2 \right), \quad (3.10)$$

into the distribution function  $F(E, L_z^2)$  and transforming to the Sun's rest frame yields

$$\begin{aligned} F_s(E, L_z^2) = & [AR^2(v_\phi + v_s)^2 + B] \\ & \times \frac{\exp \left\{ -\frac{2}{v_0^2} (v_r^2 + v_\theta^2 + (v_\phi + v_s)^2) \right\}}{(R_c^2 + R^2 + z^2/q^2)^2} \\ & + C \frac{\exp \left\{ -\frac{1}{v_0^2} (v_r^2 + v_\theta^2 + (v_\phi + v_s)^2) \right\}}{(R_c^2 + R^2 + z^2/q^2)}. \end{aligned} \quad (3.11)$$

Since  $v^2 = v_R^2 + v_z^2 + v_\phi^2$ , one can simplify this to depend only on  $v$  and the angle  $\alpha$  between the velocity and the azimuthal direction. Plugging in for the local coordinates  $(R, z) = (R_0, 0)$ , one obtains the more convenient form,

$$\begin{aligned} f(v, \alpha) = & [AR_0^2(v \cos \alpha + v_s)^2 + B] \\ & \times \frac{\exp \left\{ -\frac{2}{v_0^2} (v^2 + 2v_s v \cos \alpha + v_s^2) \right\}}{(R_c^2 + R_0^2)^2} \\ & + C \frac{\exp \left\{ -\frac{1}{v_0^2} (v^2 + 2v_s v \cos \alpha + v_s^2) \right\}}{(R_c^2 + R_0^2)}, \end{aligned} \quad (3.12)$$

where the  $q$  dependence is still implicit in the coefficients. Therefore, the local speed distribution function needed for calculation of the dark-matter detection rate is

$$f_1(v) = \frac{\int_0^\pi f(v, \alpha) v^2 \sin \alpha \, d\alpha}{\int_0^\infty \int_0^\pi f(v, \alpha) v^2 \sin \alpha \, d\alpha \, dv}. \quad (3.13)$$

The top panel in Fig. 2 shows the speed distributions  $f_1(v)$  for the nonrotating halo for  $q = 1, 0.85,$  and  $0.707$ .

### B. Maximally Corotating and Counterrotating

The calculation of the speed distribution for a rotating halo proceeds in the same fashion. However, for the maximally corotating case, the DF in the Sun's rest frame is

$$F_{+s}(E, L_z^2) = \begin{cases} F_s(E, L_z^2), & v_\phi > -v_s; \\ 0, & v_\phi < -v_s, \end{cases} \quad (3.14)$$

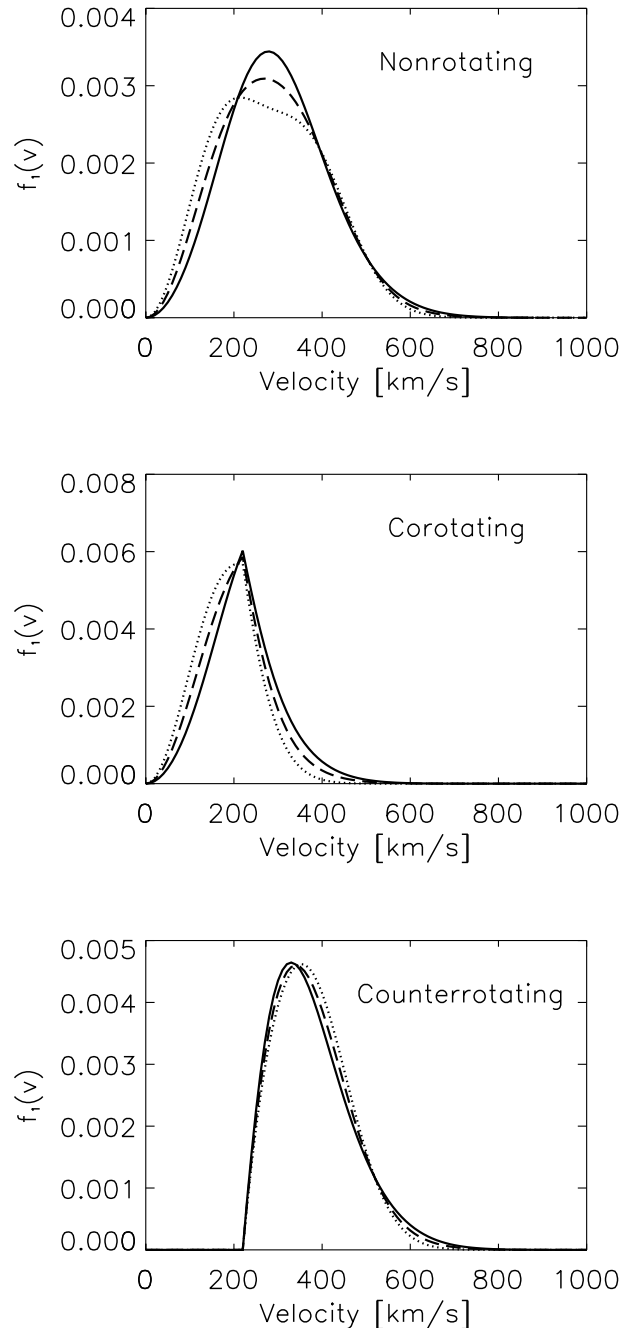


FIG. 2. Local speed distributions  $f_1(v)$  for nonrotating, maximally corotating, and maximally counterrotating models with  $q = 1$  (solid curves),  $q = 0.85$  (dashed curves), and  $q = 0.707$  (dotted curves) and with  $v_s = 220$  km/s.

and for the maximally counterrotating model, the DF in the Sun's rest frame is

$$F_{-s}(E, L_z^2) = \begin{cases} 0, & v_\phi > -v_s; \\ F_s(E, L_z^2), & v_\phi < -v_s. \end{cases} \quad (3.15)$$

The middle and bottom panels in Fig. 2 show the speed distributions  $f_1(v)$  for the maximally-corotating and counterrotating models, respectively, again for  $q = 1, 0.85,$  and  $0.707$ . Note that there are no particles with  $v < v_s$  for the maximally counterrotating model. Also, the steep rise in  $f_1(v)$  near  $v = 0$  for the  $q = 0.707$  corotating model arises because there are more particles in nearly circular orbits with velocities  $v_s$ —nearer to 0 in our frame—in this model than in the  $q = 1$  model. The maximally rotating models have a spin parameter  $\lambda = 0.18$  which is significantly larger than the spin parameters  $\lambda \simeq 0.05$  expected from galaxy-formation models [11]. Therefore, realistic speed distributions should lie somewhere between these two and closer to that for the nonrotating model.

#### IV. TOTAL AND DIFFERENTIAL DIRECT-DETECTION RATES

Fig. 3 shows the differential detection rates  $dR/dQ$  for spherical and flattened nonrotating and maximally corotating and counterrotating models. It is seen that flattening has a weak effect on the predicted differential-detection rate. Bulk rotation (especially counterrotation) has a somewhat stronger effect on the differential rates. Therefore, the shape of the nuclear recoil spectrum could provide information on whether the halo is rotating or not, and this could be useful for constraining galaxy-formation models.

Fig. 4 shows the total detection rate (assuming no thresholds) for nonrotating and maximally corotating and counterrotating models as a function of the flattening parameter  $q$ . The detection rate increases roughly as  $q^{-1}$  independent of the rotation. The larger incident WIMP velocities in counterrotating models leads to a stronger form-factor suppression. This is the leading factor in accounting for the decrease in the event rate in counterrotating models and *vice versa* for corotating models. Maximal rotation can change the event rates by roughly 30%. However, the spin parameters expected on theoretical grounds are generally smaller than a third of that for our maximally rotating halos. Therefore, the most plausible values for the bulk rotation should yield detection rates within 10% of those for the canonical nonrotating model.

The  $q$  dependence of the local halo density can be derived from Eq. (3.4), and Fig. 5 shows that it scales very nearly as  $q^{-1}$ . Fig. 6 shows the detection rate scaled by the local halo density as a function of  $q$ . These two Figures illustrate that the change in the velocity distribution from flattening has essentially no effect on the

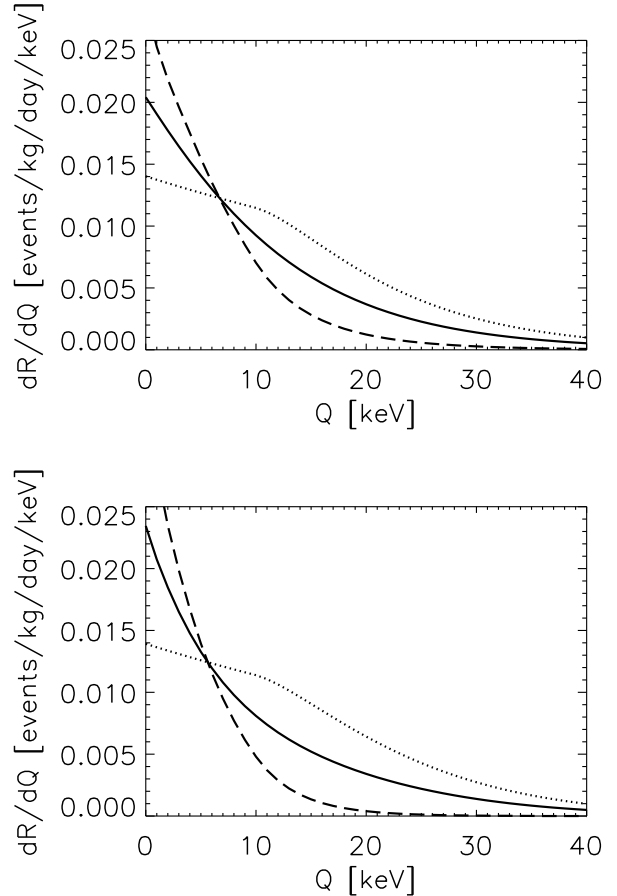


FIG. 3. Differential detection rates for Evans's models  $q = 1$  (top) and  $q = 0.707$  (bottom) with no net rotation (solid), maximal corotation (dashed), and maximal counterrotation (dotted).

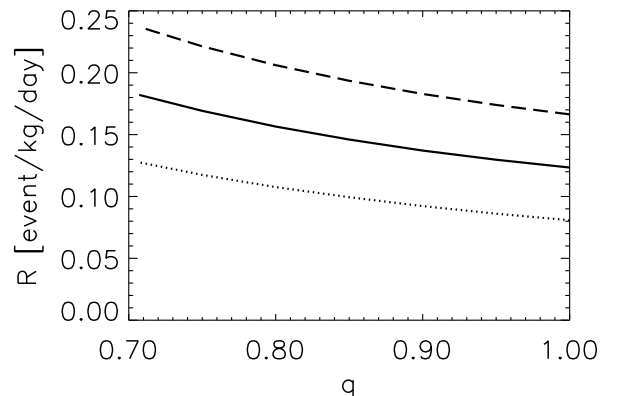


FIG. 4. Total detection rate as a function of halo flattening  $q$  for nonrotating (solid), maximally corotating (dashed), and maximally counterrotating (dotted) halos.

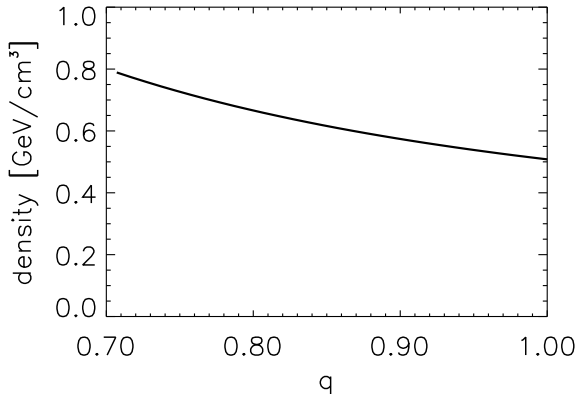


FIG. 5. Local halo density as a function of the flattening  $q$ .

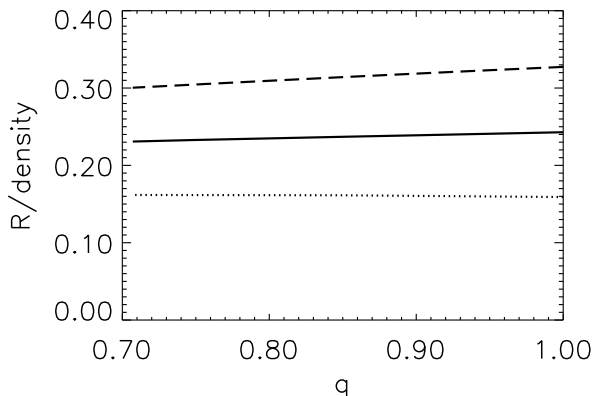


FIG. 6. Velocity dependence (i.e., the detection rate scaled by the local halo density) of the total detection rate as a function of the flattening  $q$  for nonrotating (solid), maximally corotating (dashed), and maximally counterrotating (dotted) halos.

dark-matter detection rate. Heuristically, halo particles move in the same gravitational potential as the Sun, and the velocity dispersion of any species is fixed by the potential. Our calculations contradict the claims of Cowsik et al. [14] and verify the arguments of Refs. [15].

For these calculations, we have used a WIMP with only scalar interactions of mass  $m_\chi = 100$  GeV and  $\sigma_0 = 4 \times 10^{-36}$  cm<sup>2</sup> and a Germanium target nucleus. We have checked that our conclusions do not change if we use a different WIMP mass and/or target nucleus. We have also checked that this conclusion is independent of the details of the assumed rotation curve: The velocity dispersion is essentially independent of the flattening in models where the halo contribution to the local rotation curve is higher or lower than that which we have used here, either because of different measured rotation speeds, or because of a different disk/bulge contribution.

## V. RADIAL PROFILE

Let us now consider the effect of possible variation in the radial profile in spherical halo models. Heuristically, galaxy formation results in a cored isothermal halo through the process of violent relaxation. However, there will realistically be some deviations from this simple physical picture for halo formation. For example, the collapse of baryonic matter in the Galaxy might affect this process. Empirically, the evidence for flattened spiral-galaxy halos suggests some departure from the simple picture. Therefore, even if we consider only spherical halo distributions, there is still some latitude in our choice of the precise form for the radial profile of the halo.

An empirically plausible radial profile for a spherical Galactic halo is constrained by its contribution to the Galactic rotation curve. Therefore, it should approach a constant near the core so it gives rise to a linearly rising rotation curve at small radii, and it should fall as  $r^{-2}$  at large radii to provide a flat rotation curve. The canonical profile usually used for dark-matter calculations is the so-called “isothermal” sphere (actually, the radial profile of the true cored isothermal sphere cannot be written analytically; see Ref. [13], p. 229),

$$\rho(r) = \frac{v_\infty^2}{4\pi G r_c^2} \frac{r_c^2}{r_c^2 + r^2}, \quad (5.1)$$

where  $r_c$  is a core radius which is fit to the halo contribution to the local rotation speed (and  $r$  is now the spherical radial coordinate,  $r^2 = R^2 + z^2$ ). Of course, the radial profile of the spherical Evans model,

$$\rho(r) = \frac{v_\infty^2}{4\pi G} \frac{r^2 + 3r_c^2}{(r^2 + r_c^2)^2}, \quad (5.2)$$

also has the desired properties. Yet another analytic form which might be empirically acceptable is

$$\rho(r) = \frac{v_\infty^2}{4\pi G r_c^2} \frac{r_c^2}{(r_c + r)^2}. \quad (5.3)$$

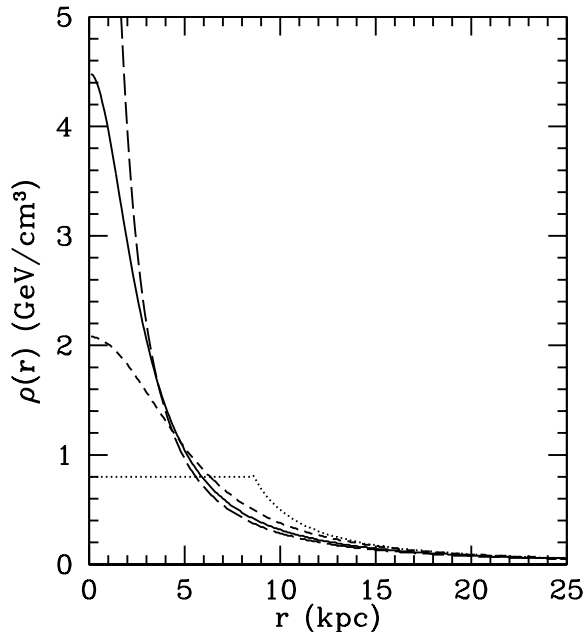


FIG. 7. The radial profile of the three spherical halo models discussed in the text. The solid, short-dash, and long-dash curves are for the canonical isothermal [Eq. (5.1)], spherical Evans [Eq. (5.2)], and alternative isothermal [Eq. (5.3)] models, respectively. The dotted curve is for the non-increasing radial profile that gives the largest local density.

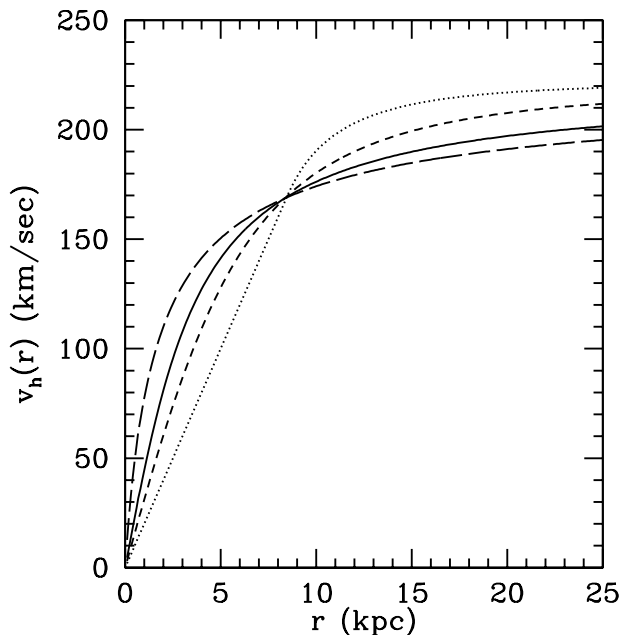


FIG. 8. Rotation curves for the spherical models shown in Fig. 7.

Keep in mind that the core radius  $r_c$  for each model must be fit to the rotation curve, and  $r_c$  for each model will be different. Suppose, as we did before, that the local rotation speed is  $220 \text{ km sec}^{-1}$  and the disk contribution is  $137 \text{ km sec}^{-1}$ . Then the local halo contribution to the rotation curve is  $170 \text{ km sec}^{-1}$  which leads to core radii  $r_c = 7 \text{ kpc}$  (as before) for the Evans model,  $r_c = 2.8 \text{ kpc}$  for the canonical isothermal sphere, and  $r_c = 0.9 \text{ kpc}$  for the alternative in Eq. (5.3). The rotation curves and radial profiles for these three models are plotted in Figs. 7 and 8 respectively. The solid, short-dash, and long-dash curves are for Eqs. (5.1), (5.2), and (5.3), respectively.

In principle, the radial profile can be fixed by the halo contribution to the rotation curve. However, measurement of the Galactic rotation curve is notoriously difficult, especially near the interior. Furthermore, the disk contribution to the rotation curve must be known to infer the halo contribution, and precise determination of the disk contribution is also difficult. Therefore, there will be significant uncertainties in any reconstruction of the halo contribution to the rotation curve from observational data.

Using our canonical values for the halo contributions to the rotation speed, we find local halo densities of  $0.43$ ,\*  $0.51$ , and  $0.38 \text{ GeV cm}^{-3}$  for the isothermal, Evans, and alternative models respectively. Therefore, although the central density of these three models may differ considerably (c.f. Fig. 7), the requirements that each yield the same halo contribution to the local rotation speed and the same asymptotic rotation speed constrain the local halo density in these models to 20%.

One could contemplate a profile with a smaller local density with a higher central density. However, a profile with a central density much greater than that in our alternative model will have a core density comparable to the Bulge density (approximately  $50 \text{ GeV cm}^{-3}$  [16]) and will therefore contradict observed Bulge dynamics. It is therefore unlikely that the local halo density can be reduced while maintaining the same halo contribution to the local and asymptotic rotation speeds. Contrariwise, one could consider a model with a larger local density and smaller core radius which still gives the same contribution to the local halo speed. Any physically reasonable radial profile should be monotonically decreasing with radius. The limiting case (a density which is constant interior to our Galactocentric radius; the dotted curve in Figs. 7 and 8) yields a density  $1.4 \text{ GeV cm}^{-3} [v_c(r_0)/v_\infty]^2$ , which results in  $0.8 \text{ GeV cm}^{-3}$  for a local halo rotation speed of  $170 \text{ km sec}^{-1}$ . Therefore, a local halo density roughly

\*This corrects the value of  $0.35 \text{ GeV cm}^{-3}$  given in Section 2.4 of Ref. [1].

twice that obtained from the canonical model is conceivable (although perhaps somewhat artificial as indicated in Fig. 7), and a local halo density  $O(10\%)$  smaller than the canonical value is also possible.

We have evaluated numerically the direct-detection rate using the DF, Eq. (3.1), for the spherical Evans model and the Maxwell-Boltzmann velocity distribution for the isothermal sphere. We find that the detection rate with the spherical Evans model is roughly 15% larger than that in the isothermal model. Therefore, the difference in detection rates can be attributed primarily to the difference in the local halo density and only secondarily to the differences in the velocity distribution. Once again—as in the case of flattening—we find that different radial profiles lead to roughly the same velocity dispersions as long as both profiles are fit to the same halo rotation speed.

## VI. CONCLUSION

Predictions for WIMP detection rates are almost always carried out assuming the dark-matter distribution to be an isothermal sphere. When fit to reasonable values of the halo contribution to the local and asymptotic rotation speeds, the canonical isothermal halo gives a local halo density  $0.25\text{--}0.5\text{ GeV cm}^{-3}$ . Its velocity distribution is Maxwell-Boltzmann with a velocity distribution fixed by the asymptotic rotation speed.

However, virtually all the empirical constraints to the halo come from its observationally inferred contribution to the Galactic rotation curve. These (still rather poorly determined) data are supplemented by some qualitative theoretical notions about the halo: i.e., that it should be more diffuse than the disk and monotonically decreasing with Galactocentric radius. Many halo distributions can satisfy these observational and theoretical constraints and still produce the same local and asymptotic rotation speeds.

In this paper, we have calculated WIMP direct-detection rates in several plausible alternatives to the canonical model. We find that if the halo is flattened with an isopotential axial ratio  $q$ , the direct-detection rate will increase by roughly  $q^{-1}$ . This increase is due primarily to the effect of flattening on the local halo density, which also increases as  $q^{-1}$ . We have used a self-consistent distribution function for a flattened halo to verify that the effects of flattening on the velocity distribution have virtually *no* effect on the detection rate. Local stellar kinematics and the thickness of gas layers suggest that halo isodensity contours may be flattened by up to a factor of 2 [8] corresponding to  $q = 0.707 - 1$  for the Evans models, which would suggest that flattening might increase the local halo density, and therefore direct-detection rates, by a factor of 1.4. However, the heuristic argument that flattening should affect the detection rate primarily through its effect on the density,

and only secondarily through its effect on the velocity distribution should also apply to a halo with ellipsoidal isodensity (rather than isopotential) contours. In such models, the local density is increased by a factor near 2 for a flattening near 2 [9].

There are no empirical constraints to the bulk rotation of the halo. A maximally corotating or counterrotating halo could increase or decrease the detection rate by 40%. However, galaxy-formation scenarios generally predict bulk rotations no more than 0.3 of maximal. Therefore, we do not expect bulk rotation to change the predicted event rates by more than 10%. Although simple galaxy-formation models suggest that a halo would corotate if it rotated at all, the existence of counterrotating disks [17] suggests that a counterrotating halo might also be plausible.

We found that in spherical models, the local density could be increased by up to a factor of two and decreased slightly with different radial profiles that still give the same local and asymptotic halo rotation speeds. In this work, we focussed on halos with axial symmetry, but it is possible that the halo may deviate somewhat from axial symmetry. However, detection rates in reasonable triaxial models also generally fall within a factor of two of the canonical detection rates [18].

We restricted our analysis to direct detection. However, similar conclusions should apply to rates for indirect detection of WIMPs via observation of energetic neutrinos from WIMP annihilation in the Sun and/or Earth. Like direct-detection rates, these rates are controlled primarily by the local halo density. Since the velocity dispersion is fixed to a large extent by the local and asymptotic rotation speeds, indirect-detection rates should not be affected by their dependence on the velocity distribution.

On the other hand, plausible deviations from the canonical isothermal sphere can lead to dramatically different fluxes of anomalous cosmic-ray antiprotons, positrons, and gamma rays from WIMP annihilation in the halo. These fluxes are determined by an integral of the *square* of the density over the entire halo. Although the local halo density does not differ too much in alternative models, the core density can differ dramatically. In particular, Fig. 7 shows that the central density can be increased perhaps by an order of magnitude over that in the canonical model. If so, then the flux of gamma rays from WIMP annihilation in the Galactic center would be increased by a factor of 100 over the fluxes predicted in canonical models.

There is also the possibility that if WIMPs are detected, the nuclear recoil spectrum might tell us about the structure of the halo. Fig. 3 shows how the recoil spectrum could be used to constrain the rotation of the halo. We have also investigated the magnitude of annual modulations in the event rate due to the Earth's orbital motion around the Sun. We found a maximally corotating halo could increase the annual modulation by a factor of 2, implying an increase in modulation amplitude



of  $O(30\%)$  for models with more realistic corotation.

### ACKNOWLEDGMENTS

We thank M. Weil for useful discussions. M.K. was supported by the D.O.E grant number DEFG02-92-ER 40699, NASA NAG5-3091, and the Alfred P. Sloan Foundation. A.K. was supported by the Columbia Rabi Scholars Program which is funded in full by the Kann Rasmussen Foundation.

- 
- [1] G. Jungman, M. Kamionkowski, and K. Griest, Phys. Rep. **267**, 195 (1996).
- [2] H. E. Haber and G. L. Kane, Phys. Rep. **117**, 75 (1985).
- [3] M. W. Goodman and E. Witten, Phys. Rev. **D31**, 3059 (1986); I. Wasserman, Phys. Rev. **D33**, 2071 (1986); K. Freese, J. Frieman, and A. Gould, Phys. Rev. **D37**, 3388 (1988); K. Griest, Phys. Rev. **D38**, 2357 (1988); FERMILAB-Pub-89/139-A (E); A. Drukier, K. Freese, and D. Spergel, Phys. Rev. **D33**, 3495 (1986).
- [4] See, e.g., J. Low Temp. Phys. **93** (1993).
- [5] J. Silk, K. A. Olive, and M. Srednicki, Phys. Rev. Lett. **55**, 257 (1985); K. Freese, Phys. Lett. **B167**, 295 (1986); L. M. Krauss, K. Freese, D. N. Spergel, and W. H. Press, Astrophys. J. **299**, 1001 (1985); L. M. Krauss, M. Srednicki, and F. Wilczek, Phys. Rev. **D33**, 2079 (1986); T. Gaisser, G. Steigman, and S. Tilav, Phys. Rev. **D34**, 2206 (1986); K.-W. Ng, K. A. Olive, and M. Srednicki, Phys. Lett. **B188**, 138 (1987); M. Kamionkowski, Phys. Rev. **D44**, 3021 (1991).
- [6] S. R. Kulkarni, L. Blitz, and C. Heiles, Astrophys. J. Lett. **259**, L63 (1982); L. Blitz, in *Dark Matter*, proceedings of the conference, College Park, MD, October, 1994, edited by S. S. Holt and C. L. Bennett (American Institute of Physics, Woodbury, 1995).
- [7] P. D. Sackett et al., Astrophys. J. **436**, 629 (1994).
- [8] R. Olling and D. Merrifield, in preparation.
- [9] E. I. Gates, G. Gyuk, and M. S. Turner, Astrophys. J. Lett. **449**, L123 (1995).
- [10] J. Dalcanton, D. N. Spergel, and F. J. Summers, Astrophys. J. **482**, 659 (1997).
- [11] J. Barnes and G. Efstathiou, Astrophys. J. **319**, 575 (1987); M. S. Warren, P. J. Quinn, J. K. Salmon, and W. H. Zurek, Astrophys. J. **399**, 405 (1992).
- [12] N. W. Evans, Mon. Not. R. Astr. Soc. **260**, 191 (1993).
- [13] J. Binney and S. Tremaine, *Galactic Dynamics* (Princeton University Press, Princeton, 1987).
- [14] R. Cowsik, C. Ratnam, and P. Bhattacharjee, Phys. Rev. Lett. **76**, 3886 (1996).
- [15] N. W. Evans, Phys. Rev. Lett. **78**, 2260 (1997); E. Gates, M. Kamionkowski, and M. S. Turner, Phys. Rev. Lett. **78**, 2261 (1997).
- [16] H. S. Zhao, D. N. Spergel, and R. M. Rich, Astrophys. J. Lett. **440**, L13 (1995).
- [17] V. C. Rubin, J. A. Graham, and J. D. P. Kenney, Astrophys. J. Lett. **394**, L9 (1992).
- [18] D. N. Spergel and D. O. Richstone, in *Dark Matter*, proceedings of the XXIIIrd Rencontres de Moriond, Les Arcs, Savoie, France, 8–15 March 1988, edited by J. Audouze and J. Tran Thanh Van (Editions Frontieres, Gif-sur-Yvette, 1988).